The role of metamorphic fluid in tectonic tremor along the Alpine Fault, New Zealand

Timothy Chapman[1], Luke A. Milan[2], and Julie Vry[3]

[1]University of New England
[2]The University of New England
[3]Victoria University Wellington

November 23, 2022

Abstract

The production of H_2O during metamorphism along active plate boundaries is inferred to contribute to low-frequency tectonic tremor seismicity. This study combines predictions from phase equilibria and mechanical modelling of coincident volume changes to investigate links of tremor with hydrofracturing and fluid migration under the actively forming Southern Alps, New Zealand. Our predicted location of metamorphic fluid production correlates with published geophysical images of inferred permeability enhancement, fluid accumulation and potential fluid flow. As the hanging-wall rocks are translated towards the surface by motion along the Alpine Fault, they can undergo metamorphic reactions that involve positive volume changes. Production of metamorphic fluids leads to hydrofracturing and the development of tremor hypocentres in regions along, and above deep reflectors of the Alpine Fault. The capacity of metamorphic rocks to generate or consume fluid along portions of the pressure–temperature path exerts a fundamental control on the distribution of stresses in the crust.

Hosted file

`supplementary.docx` available at https://authorea.com/users/546035/articles/602243-the-role-of-metamorphic-fluid-in-tectonic-tremor-along-the-alpine-fault-new-zealand

The role of metamorphic fluid in tectonic tremor along the Alpine Fault, New Zealand

Timothy Chapman[1]*, Luke Milan[1], Julie Vry[2]

[1]*School of Environmental and Rural Science, University of New England, NSW, 2351, Australia;* *timothy.chapman@une.edu.au

[2]*School of Geography, Environment and Earth Sciences, Victoria University of Wellington, 6040, New Zealand*

Keywords: metamorphic dehydration, seismicity, pore-fluid pressure, Alpine Schist, phase equilibria

Key points

- Links between metamorphic dehydration and hydrofracturing are investigated in the Southern Alps of New Zealand
- Metamorphic fluid production leads to the development of tremor hypocentres in regions along, and above deep reflectors of the Alpine Fault
- The capacity of metamorphic rocks to generate or consume fluid along portions of the *P*–*T* path exerts a control on stresses in the crust.

ABSTRACT

The production of H_2O during metamorphism along active plate boundaries is inferred to contribute to low-frequency tectonic tremor seismicity. This study combines predictions from phase equilibria and mechanical modelling of coincident volume changes to investigate links of tremor with hydrofracturing and fluid migration under the actively forming Southern Alps, New Zealand. Our predicted location of metamorphic fluid production correlates with published geophysical images of inferred permeability enhancement, fluid accumulation and potential fluid flow. As the hanging-wall rocks are translated towards the surface by motion along the Alpine Fault, they can undergo metamorphic reactions that involve positive volume changes. Production of metamorphic fluids leads to hydrofracturing and the development of tremor hypocentres in regions along, and above deep reflectors of the Alpine Fault. The capacity of metamorphic rocks to generate or consume fluid along portions of the pressure–temperature path exerts a fundamental control on the distribution of stresses in the crust.

PLAIN LANGUAGE SUMMARY

As continents collide rocks traverse through the mountain belt and undergo prograde metamorphism. This releases water that has been bound in minerals in the rocks because of the effects of both heating and decompression. The production of water from these rocks contributes to the generation of low-frequency and low-energy earthquakes. This study is the first to couple mineral phase equilibria of dehydration processes with mechanical modelling of the resulting volume changes to investigate the potential links between hydrofracturing and seismicity under the Southern Alps of New Zealand. The positive volume changes that accompany dehydration during exhumation can induce hydrofracturing and the development of low frequency earthquakes at mid-crustal depths.

INTRODUCTION

In active collisional plate boundaries, such as the Alpine Fault in New Zealand, zones of high pore fluid pressures at depth are correlated with regions of high seismic reflectivity and electrical conductivity (Wech et al., 2012). These anomalies mark domains of metamorphic dehydration and the accompanying development of fluid connectivity (Alvizuri & Hetényi, 2019; Hetényi et al., 2020). Elevated fluid–rock ratios can lower effective stress, leading to shear failure and hydrofracturing (Hobbs & Ord, 2018). The development of high pore fluid pressures in domains experiencing shearing can thus contribute to the generation of non-volcanic tectonic tremor – a low-frequency seismicity that is linked to slow slip in the crust (Obara, 2002; Shelly et al., 2007; Thomas et al., 2009; Wech et al., 2012). The operation of low-energy slip is also dependent on the rate of state of friction in the crust (Shelly et al., 2007; Bernaudin & Gueydan, 2018). In detail, the development of tremor hypocentres will be influenced by the capacity of metamorphic rocks to generate fluid along different parts of their *P*–*T* path (Fagereng et al., 2011a).

Hydrofracturing in the crust is caused by increases in fluid pressure that are intrinsically dependent on volume changes generated by deformation or mineral reactions that create capacity for fluid movement (Yardley, 1981; Walther & Orville, 1982; Etheridge, 1983; Connolly et al., 2010). The generation of metamorphic fluids has traditionally been attributed to the effects of progressive heating, with partial fluid consumption accompanying subsequent cooling (Yardley, 1981; Fagereng & Diener, 2011b). This ignores the potential for metamorphic dehydration to occur during the early exhumation history (Vry et al., 2010). The actual production of fluid in the crust will depend on the bulk-rock compositions involved, and the slopes, in *P*–*T* space, of the metamorphic reactions that those rocks encounter as they travel along their individual *P*–*T* paths (e.g. Guiraud et al., 2001). Previously metamorphosed rocks may be capable of releasing less water during subsequent events, depending on the metamorphic *P–T* path (Guiraud et al., 2001; Clarke et al., 2006; Tenczer et al., 2006). Any metamorphic fluid produced can induce fluctuations in effective stress that contribute to cycles of slip failure and tectonic tremor (Bernaudin & Gueydan, 2018).

The Southern Alps of New Zealand represents an ideal location in which to study the interplay of metamorphism and its association to stress distribution and tremor in the crust. Results of previous studies in the area have yielded a remarkable abundance of high-resolution geophysical data, which record regions of metamorphic fluid generation and developing zones of fluid connectivity (Wannamaker et al. 2002; Stern et al., 2007; Wech et al., 2012; Chamberlain et al., 2014). These domains correspond to observations of veining, deformation and in places gold mineralisation in the exhumed portions of the orogen, which are consistent with predictions from phase equilibria modelling of metamorphic fluid production (Koons et al., 1998; Little et al., 2002; Wightman et al., 2006; Toy et al., 2010; Vry et al., 2010). In this study, we employ for the first time a coupled mechanical and phase equilibria modelling approach to investigate the links between metamorphic fluid generation and tectonic tremor along, and in, the hanging-wall above the Alpine Fault on the South Island of New Zealand (Fig. 1).

GEOLOGICAL SETTING OF SOUTHERN ALPS

The Southern Alps orogen on the South Island of New Zealand (Fig. 1) is one of the most active mountain belts in the world. The orogen is forming by the ongoing oblique continental convergence of the Pacific Plate and the Australia Plate, at ~40 mm yr^{-1} (De Mets et al., 2010). Dextral-reverse slip on the southeast-dipping Alpine Fault is accompanied by burial, uptilting, rapid uplift, and erosional exhumation of the Alpine Schist at ~10 mm yr^{-1} (Norris et al., 1990). The tilted section comprises a Mesozoic accretionary complex comprised mainly of metamorphosed greywacke, with minor pelite, calc-schist, and mafic rock types

(Mortimer, 2004). The metamorphic grade increases towards the fault over distances of 15–20 km (Fig. 1), from prehnite–pumpellyite facies in the east to greenschist and amphibolite facies conditions nearer the fault (Grapes & Watanabe, 1992; Vry et al., 2004; Briggs et al., 2017).

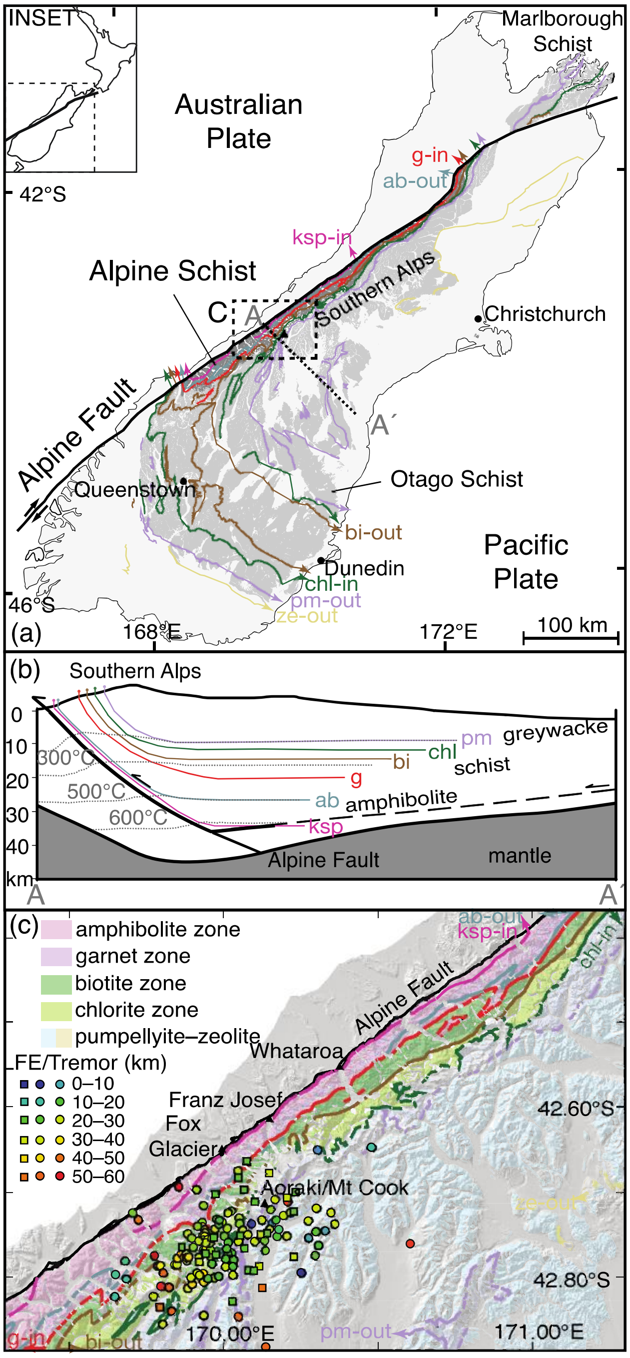

Figure 1. (a) Configuration of the Alpine Fault on the South Island of New Zealand, including the distribution of the Alpine and Otago Schist and their metamorphic isograds (adapted from Heron, 2018). (b) Cross section (A–A´) displays the distribution of mineral

isograds and isotherms in the Alpine Schist beneath the Southern Alps. (c) Detailed geological map of the Mt Cook and Franz-Josef/Fox Glacier area displaying the locations and depths of tremor and low frequency earthquake (LFE) hypocentres (Wech et al., 2012, 2013; Chamberlain et al., 2014; Baratin et al., 2018).

In the Southern Alps minerals associated with the Jurassic orogeny (Otago Schist) were effectively consumed by greenschist and amphibolite grade metamorphism during the Late Cretaceous (*c*. 97–64 Ma) and late Cenozoic (6 Ma–present: Vry et al., 2004; Briggs et al., 2017). The younger events affecting the Alpine Schist involved higher heat flow along a clockwise P–T path. Initial prograde burial from T = 300–380˚C and P = 0.25–0.35 GPa to T of 450–480˚C at P of 0.8 GPa (S_2) occurred in the Cretaceous (Vry et al., 2004). The dominant Cenozoic high-grade mineral assemblages define steeply dipping fabrics (S_3) and isograds that strike obliquely to the Alpine Fault (Grapes & Watanabe, 1992; Grapes, 1995; Little et al., 2002; Toy et al., 2010; Beyssac et al. 2016).

The Cenozoic Southern Alps orogenic event involves fluid generation, with new mineral growth accompanying peak metamorphism (T of 570–650˚C and P of 0.9–1.2 GPa) and subsequent near-isothermal uplift of rocks near (~10 km) the Alpine Fault (Batt & Braun, 1999; Little et al., 2002, Vry et al., 2004, Menzies et al., 2016). Recent thickening of the Southern Alps contributed to widespread amphibolite grade overprinting of the Alpine Schist in the crustal root (Ring et al., 2019). The clearest representation of this event are mylonites exposed within 1–2 km of the Alpine Fault that record amphibolite grade metamorphism at *c*. 10–14 Ma (Little et al., 2002). Young *c*. 1–2 Ma ^{40}Ar–^{39}Ar and Rb–Sr ages in muscovite and biotite record the rapid ongoing cooling (T of 450–500˚C) and exhumation (from depths of 10–15 km) of the Alpine Schist to shallower conditions (Ring et al., 2019). Metamorphism is presently ongoing as rocks are translated along the Fault 'ramp' from the lower crust to the surface.

Phase Equilibria and Mechanical Modelling

Calculated phase equilibria for the Alpine Schist provide a basis for quantifying the formation of H_2O-rich fluid and the mechanical pore fluid pressure (Fig. 2). Phase equilibria modelling of a representative Alpine Schist bulk-composition was performed using THERMOCALC version 3.47 in the MnNCKFMASHTO chemical system (MnO–Na_2O–CaO–K_2O–FeO–MgO–Al_2O_3–SiO_2–H_2O–TiO_2–O) utilising the internally consistent thermodynamic dataset 6.2 (updated 6th February 2012: Holland & Powell, 2011) and activity composition models as outlined in the supplement.

The inferred *P*–*T* history of the Alpine Schist relates primarily to a Cretaceous prograde burial geotherm that approaches gradients of 20˚C per km (Fig. 2a: Vry et al., 2008). Renewed metamorphism starting in the Miocene includes peak-*P*–*T* and associated near isothermal decompression to define the 'Cenozoic' portion of the *P*–*T* loop (Grapes & Watanabe, 1992; Vry et al., 2010; Beyssac et al., 2016). Mineral assemblages involving garnet, plagioclase, clinozoisite, and hornblende preserved in components of calc-schist and greyschist are consistent with limited heating (30–50˚C) during decompression (~0.5 GPa) and the onset of mylonitization (Fig. S4: Ring et al., 2019). Alpine Schist distal from the Alpine Fault experienced decompression at successively lower *T* during their exhumation from differing depths (Figs 2a & 2b). Partial retrogression in the late Cenozoic occurred at greenschist facies conditions, though most rock types retain assemblages from higher-*T* that define the metamorphic field array (Grapes & Watanabe, 1992; Vry et al., 2008). Detailed petrographic relationships that constrain the *P*–*T* path and the phase equilibria are provided in the supplement.

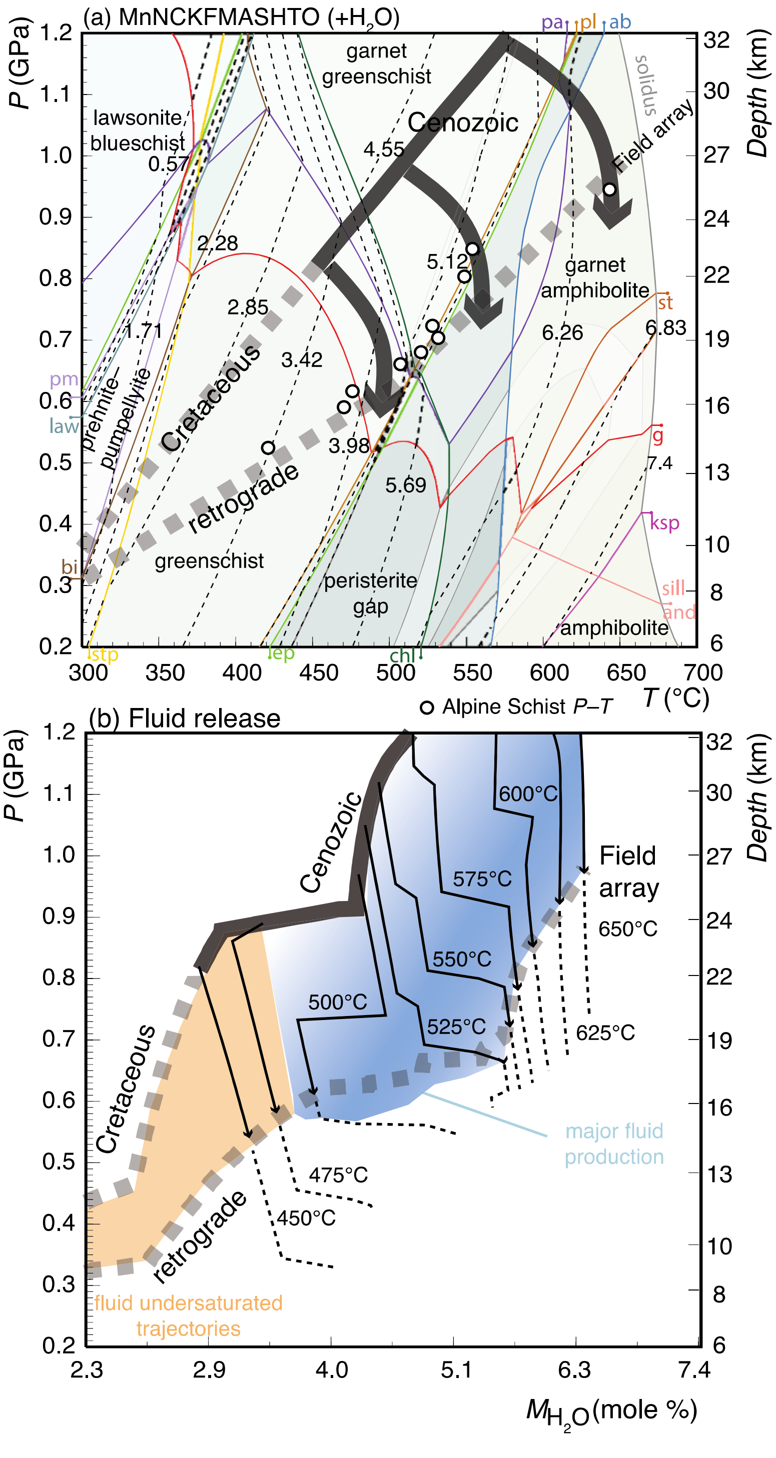

Figure 2. (a) P–T pseudosection for the Alpine Schist showing conditions of the metamorphic facies and isopleths of H_2O (mole %, detail in Figs S1 & S2). Thick lines represent the 'Cenozoic' and dashed lines the 'Cretaceous' portions of the P–T path. White filled circles are the exposed P–T conditions of the schist (after Grapes & Watanabe, 1992). (b) Predicted fluid generated (mole %) during prograde, peak, and decompression metamorphism of the Alpine Schist. The decompression history is shown by the black lines until they intersect the field array. Fluid is released during decompression to depths of 8–22 km at T of 450–600˚C.

Pre-conditioning from the Cretaceous metamorphism induces fluid-poor decompression for schists formed at T <470˚C.

Extracted molar volumes of phases along the *P–T* path of the Alpine Schist (Figs 2 & S2) enables mechanical calculations of the evolving pore fluid pressures associated with the effects of thermal expansivity and compressibility between the fluid and solid framework. The quantification of pore-fluid pressure (P_f) over a certain *PT* increment (δPT) was undertaken following equations of Etheridge et al. (2020):

$$\frac{P_{f(PT+\delta PT)}}{P_{f(PT)}} = \frac{V_{f(PT)} + (\delta V_{f(PT+\delta PT)} + \delta V_{s(PT+\delta PT)})}{V_{f(T)}} \qquad (1)$$

where $V_{f(PT)}$ is the molar volume fraction of fluid corrected for the non-linear equation of state and mode; $\delta V_{f(PT+\delta PT)}$ is the increase fluid molar volume due to δPT; $\delta V_{s(PT+\delta PT)}$ is the change in molar volume of the solid phases ($-\delta V_{s(PT+\delta PT)}$ representing the transient change in porosity still in equilibrium with the system: Powell et al., 2019); $P_{f(PT)}$ and $P_{f(PT+\delta PT)}$ are the respective fluid pressures (Fig. 3). As the phase equilibria modelling is a closed system approach, each increment was based only on the change in molar volume of the reaction products (Fig. S2 shows the progressive change of both). Differences in the thermal expansivity and compressibility between the fluid and solid framework is accounted for by using internal thermodynamically calculated molar volumes of each phase (e.g., Chapman et al., 2019). A closed system approach in terms of excess H_2O is reasonable as metamorphic progress in the Alpine Schist is consistent with fluid saturated assemblages.

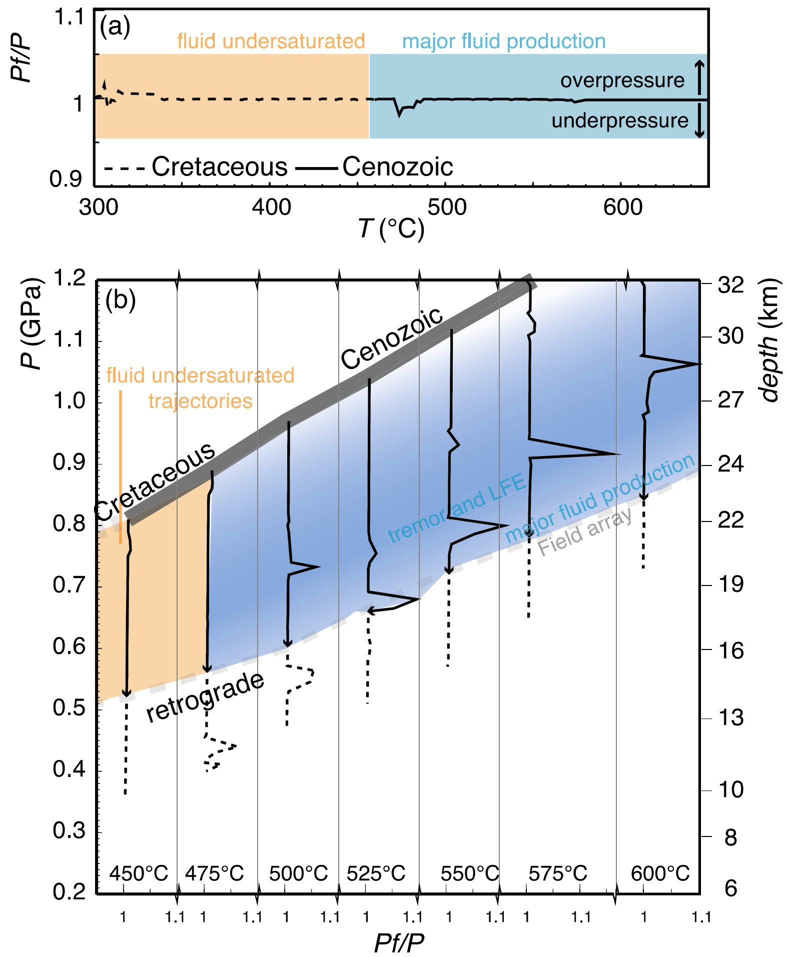

Figure 3. (a) Pore fluid pressure along the prograde and peak P–T path of the Alpine Schist defining domains of fluid undersaturation and production. (b) Pore fluid factor during the isothermal decompression as black lines until they intersect the field array or retrograde trajectories. Each isotherm represents its own portion of a pore fluid factor diagram that are collectively stacked. Pronounced overpressure occurs during decompression at depths of 15–30 km (shaded blue). Cooler portions of the Alpine Schist are defined by fluid undersaturation and act as sinks (orange regions).

METAMORPHIC FLUID PRODUCTION

The interplay between prograde metamorphism and deformation in the crust is a key controlling agent for fluid production and migration (Fagereng & Diener, 2011a). The recorded peak mineral assemblages in Miocene portions of the Alpine Schist are consistent with prograde burial to amphibolite facies conditions (500–650˚C, P = 0.9–1.2 GPa: Fig. S4) greater than those experienced during the Cretaceous (T = 450–480˚C, P = 0.8 GPa: Vry et al., 2004; Ring et al., 2019). Closure of mineral isotopic systems also support rapid uplift with limited cooling (100–150˚C) of the rocks to depths of 10–15 km in the period of *c.* 2–12 Ma (Little et al., 2005; Ring et al., 2019). The recent heating and decompression of the exposed portions of the Alpine Schist involve a *P*–*T* loop that continually intersects H_2O isopleths of higher value (Fig. 2a). In the Southern Alps of New Zealand pronounced fluid generation (20–50% of the total fluid capacity) occurs therefore both as a consequence of metamorphism during burial, and also exhumation. The production of fluid via latent heating during decompression compounds typical interpretations of fluid sources during active orogeny (Vry et al., 2010; Menzies et al., 2016).

The low electrical resistivity anomaly adjacent to the Alpine Fault (Fig. 4b: Wannamaker et al., 2002; Stern et al., 2007) is consistent with our interpretations of the recent record (*c*. present–6 Ma) of rocks transitioning across the boundary of the greenschist and amphibolite facies during decompressive unroofing (*T* of ~450–600˚C at *P* of ~0.5–1.0 GPa: Fig. 2). The boundary is delineated by the breakdown of epidote and chlorite, with or without paragonite near the albite–oligoclase peristerite gap (Fig. 2a). Together the reactions contribute the release of 30% of the total fluid capacity (~3.2 mole % of H_2O) within a narrow depth interval as the wedge is exhumed (~10 km: Figs 2b & 4a). The spatially defined locations of this dehydration in the crust are consistent with observations from equivalent rocks now exposed between the Alpine Fault and the main divide of the Southern Alps (Fig. 1). Clear evidence for the escape of significant amounts of fluid exists in the form of thick arrays of regularly spaced, vein infilled faults inferred to have formed at *T* of 450–500˚C and depths of ~18–23 km are now at the surface in the central Southern Alps (Little et al., 2005; Wightman et al., 2006). The deformed veins formed during exhumation (*c*. 4 Ma) and derived fluid from the surrounding or deeper portions of the dehydrating Alpine Schist (Wightman et al., 2006). Additionally, the Alpine Schist adjacent to the fault contains grain-boundary tubules in garnet porphyroblasts that were generated by the breakdown of clinozoisite and chlorite to form oligoclase (Fig. S1: Grapes & Watanabe, 1984; Grapes, 1995; Vry et al., 2001). Some of these domains are accompanied by instances of substantial localised retrogression to chlorite-rich assemblages (Vry et al., 2001).

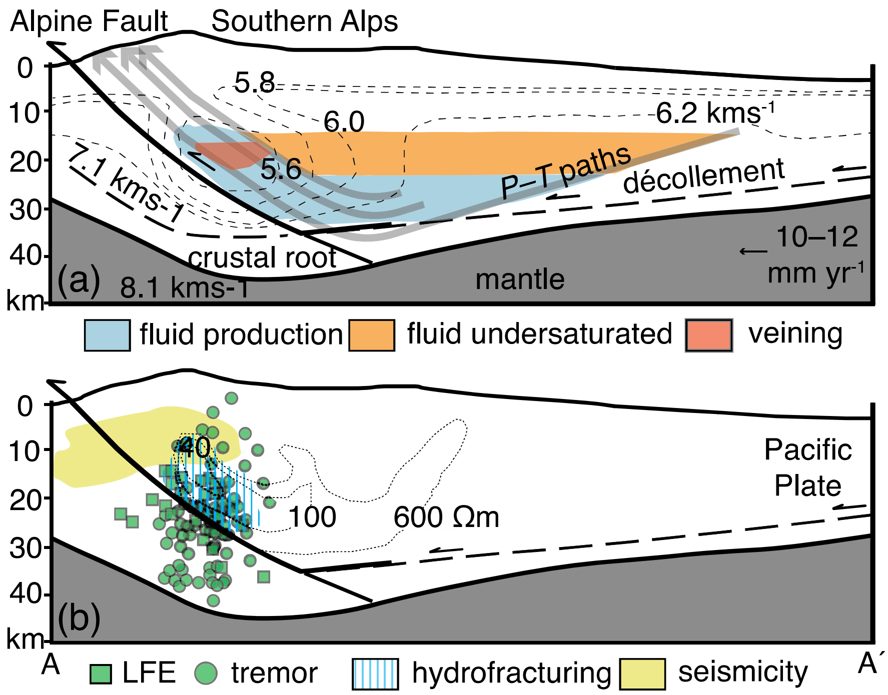

Figure 4. Schematic cross section (A–A´ Fig. 1) of the Southern Alps displaying (a) the predicted domains of fluid production, undersaturation, and veining (Wightman et al., 2006). The arrows represent P–T paths of Alpine Schist experiencing decompression at T of 600, 550 and 500˚C. The predictions of fluid production and veining correspond to observations of seismic reflectors (a: Stern et al., 2007) and (b) the distribution of hydrofracturing, magnetotelluric anomalies (Wannamaker et al., 2002) and tectonic tremor and low frequency earthquake hypocentres (Wech et al., 2012, 2013; Chamberlain et al., 2014; Baratin et al., 2018).

The active extent of prograde dehydration in the unexposed portions of the Alpine Schist is limited (15–20% fluid production: Fig. 4), but consistent with the lateral protrusion of resistivity anomalies towards the eastern portions of the crust beneath the Southern Alps (Eberhart-Phillips et al., 2008). It is mostly assumed that this dehydration is related to the attainment of *P*–*T* conditions near the discontinuous reactions at the upper-*T* end of the greenschist facies (Fig. 2). The existence of metamorphic mineral assemblages in the exposed Alpine schist that are largely inherited from the Late Cretaceous, means that the rocks had already undergone significant prior dehydration and potential tremor (e.g. Fagereng et al., 2018). The exposed field array supports fluid-saturated progress across pumpellyite, chlorite and garnet zones (Grapes & Watanabe, 1992; Vry et al., 2008). The early prograde dehydration occurred in portions of the Cretaceous Alpine Schist and the Jurassic Otago Schist inducing veining and mineralisation (Mortimer et al., 2004). This pre-conditioned history presents limitations to subsequent fluid production rates of the Alpine Schist without additional heating or subsequent ingress; any meteoric fluid flow is restricted to shallow levels (<10 km: Fig. 2b: Koons & Craw, 1991; Menzies et al., 2016). Fluid production of >1.5 mol.% in these pre-condition circumstances is only feasible via the crossing of H_2O isopleths of higher value than those obtained at the peak metamorphic conditions (Figs 2a & b: Guiraud et al., 2001; Fagereng & Diener, 2011b). The recent metamorphic progress starting from at *c*. 6 Ma, across the peristerite gap and into amphibolite facies conditions is consistent with renewed fluid production in the crustal root and during decompression along the Alpine Fault.

Portions of the Alpine Schist distal to the Alpine Fault that had previously attained conditions in the *T* range of 300–450˚C during the Cretaceous are predicted to follow fluid-undersaturated exhumation paths during the ongoing Southern Alps orogeny, retaining chlorite, sodic white mica and garnet greenschist assemblages (Figs 2 & 3: Grapes & Watanabe, 1992; Vry et al., 2008). The assemblages are consistent with the limited record of metamorphism initiated in the Miocene in distal portions of the Alpine Schist. The defined occurrences of these currently fluid-poor packages in the mid-crust are consistent with identified high-seismic velocity domains beneath the main divide of the Southern Alps (Fig. 4: Eberhart-Phillips et al., 2008).

Preserving fluid undersaturated rock along lower *T* (300–450˚C) portions of the decompression evolution, would control the direction of vertical and lateral fluid flow in the central and eastern portions of the Southern Alps (Fig. 4: Wannamaker et al., 2002; Stern et al., 2007). Fluid-undersaturated domains with lower pore-fluid pressures act as local sinks for H_2O migration, pumped from adjacent hotter portions of the crust, if mechanical processes can propagate porosity (Fig. 3: Connolly, 2010; Hobbs & Ord, 2018; Bernaudin & Gueydan, 2018). The migration of fluid ~10–15 km towards the east of the fault is consistent with geophysical resistivity anomalies (Fig. 4) and weakened crustal domains that have focussed back-shearing and retrogression to chlorite-rich assemblages (Fig. 3: Koons et al., 1998; Vry et al., 2001; Little et al., 2002).

INITIATING TREMOR EPISODES

The location of low frequency tremor seismicity in active plate boundaries is well correlated to slow slip domains in the crust that retain high pore-fluid pressures (Obara, 2002; Shelly et al., 2007). In the Southern Alps tremor hypocentres are mostly focussed at depths of 10–30 km near deep reflectors of the Alpine Fault, or the inferred extensions of the plate boundary (Wech et al., 2012; Chamberlain et al., 2014; Baratin et al., 2018). Periodicity of tremor events along deep-seated fault zones is commonly ascribed to slip failure in rock piles experiencing metamorphic devolatilization, inducing lower effective stress and cycles of hydrofracturing and fluid pumping (Fagereng & Diener, 2011a; Chamberlain et al., 2014; Bernaudin & Gueydan, 2018; Thomas et al., 2009). Such behaviour is consistent with geophysical and geological observations along the Alpine Fault (Wech et al., 2012).

The depth of fluid production and hydrofracturing in the Southern Alps is temperature sensitive. Domains of fluid production correspond closely to hypocentres of tremor seismicity and fault reflectors at depths of 10–30 km along isotherms of 450–600˚C in the hanging wall (Figs 1, 3 & 4: Wech et al., 2012). Most zones of prograde dehydration in the crustal root are distal (eastwards) from active slip (Figs 3a & 4). Additional dehydration in the footwall is consistent with the intersection of the greenschist–amphibolite transition at depth, though is more difficult to validate on account of the active burial of the Palaeozoic metasedimentary sequence (Menzies et al., 2016).

In regions of high fluid to rock ratios (high effective stress) brittle shear failure is enabled at lower differential stress, as hydrological conditions approach lithostatic values (Hobbs & Ord, 2018). For commonly determined rock strengths in anisotropic foliated rocks of transpressional settings, like the Alpine Fault, the pore-fluid pressure need only exceed lithostatic values by 0.005–0.01 GPa to induce brittle failure (Fig. 3: Etheridge et al., 1983). This contrasts with low-porosity rocks at the same imposed conditions that mostly deform by elastic mechanisms at the prevailing hydrostatic conditions (Cox, 2010; Fagereng et al., 2014, 2018).

Pore fluid pressure in metamorphic rocks is inherently controlled by the amount of fluid produced during dehydration and the accompanying volume change of fluid and solids during reaction or strain. The change in volume of the reaction must be accommodated by dissipation from concomitant deformation that takes a net dilatational ($\Delta V>0$) or compressional ($\Delta V<0$) form depending on the P–T slope of the reaction. Rapid hydrofracturing is induced when the pore-fluid pressure exceeds the tensile strength of the rock during these dilatational reactions (Etheridge et al., 1983, 2020; Connolly, 2010). In the Alpine Schist this requires overpressures of 0.4% (0.005 GPa > confining P) to intersect the brittle shear failure envelope (Fig. 3: Cox, 2010; Etheridge et al., 2020). The positive dP/dT form of the epidote dehydration reaction predicted to be experienced by the exhuming metamorphic pile at T >450˚C would induce expansion of pore fluid forces greater than the tensile rock strength (σ_3), suitable to induce hydrofracturing and fluid migration (Fig. 3). The drained system would then relax back to the P of the confining lithostatic load as the rock passes through the orogen. Evidence for the breakdown of epidote is supported by the restriction of clinozoisite inclusion to garnet cores and the prevalence of oligoclase in the matrix of Alpine mylonites (Ring et al., 2019). Comparatively, epidote forms part of the peak mineral assemblages in the Cretaceous schists to the east (Fig. S1: Vry et al., 2004). The location of zones of fluid overpressure and hydrofracturing would propagate to shallower depths with cooler T as the rocks passively move to the surface (Fig. 3b). The distribution of tremor hypocentres in the central Southern Alps is consistent with domains of rapid exhumation of the Alpine Schist (Little et al., 2005). By coupling models for dehydration reactions and volume changes, we can demonstrate the likelihood and location in the crust where tectonic tremors can be predicted during uplift.

The transpressional tectonic regime of the Alpine Fault would support multiple failures, as the confining pressure is continually exceeded during the dehydration event (Koons et al., 1998; Etheridge et al., 2020). Instantaneously after failure, both fluid pressure and differential stress will be lowered by fracture porosity and seismic or aseismic stress relief. Each individual episode of hydrofracturing would be followed by recovery, then repeated multiple times during ongoing fluid production as the rocks travel through the orogen (Fig. 3: Cox, 2010). Shear failure could also be initiated at constant high pore fluid pressures by increasing the differential stress. In exhumed high-strain mylonite the occurrence of extensive quartz–biotite vein sets, and local chlorite-rich domains is consistent with the progression of these cycles of reaction, hydrofracturing, deformation and tremor at greenschist facies conditions (Vry et al., 2001; Toy et al., 2010; Ring et al., 2019). Dynamic feedbacks between these processes at the grain- to rock-scale are considered to be additional drivers of the cyclicity of tremor episodes (Thomas et al., 2009; Bernaudin & Gueydan, 2018).

ACKNOWLEDGMENTS

T. C. and L. A. M. received funding from the University of New England. J. K. V. acknowledges support from the School of Geography, Environment and Earth Sciences that helped enable a visit to the University of New England in 2019. M. Etheridge is thanked for stimulating discussions on the topic. Comments from S. Schorn and two anonymous reviewers substantially improved the work.

Data availability statement

Thermodynamic data used in the study is available in the reference Holland & Powell (2011, 10.1111/j.1525-1314.2010.00923).

REFERENCES CITED

Alvizuri, C., and Hetéyni, G., 2019. Source mechanisms of a lower crust earthquake beneath the Himalayas and its possible relation to metamorphism. Tectonophysics, 769, 128153.

Baratin, L-M., Chamberlain, C. J., Townend, J., and Savage, M. K., 2018. Focal mechanisms and inter-event times of low-frequency earthquakes reveal quasi-continuous deformation and triggered slow slip on the deep Alpine Fault. Earth and Planetary Science Letters, 484, 111–123.

Bernaudin, M., and Gueydan, F., 2018. Episodic tremor and slip explained by fluid-enhanced microfracturing and sealing. Geophysical Research Letters, 45, 3471–3480, doi: 10.1029/2018GL077586.

Beyssac, O., Cox, S. C., Vry, J., and Herman, F., 2016. Peak metamorphism temperature and thermal history of the Southern Alps (New Zealand). Tectonophysics, 676, 229–249.

Briggs, S. I., Cottle, J. M., and Smit, M. A., 2017. Record of plate boundary metamorphism during Gondwana breakup from Lu–Hf garnet geochronology of the Alpine Schist, New Zealand. Journal of Metamorphic Geology, 36, 821–841.

Chamberlain, C. J., Shelly, D. R., Townend, J., and Stern, T. A., 2014. Low-frequency earthquakes reveal punctuated slow slip on the deep extend of the Alpine Fault, New Zealand. Geochemistry, Geophysics, Geosystems, 15, 2984–2999, doi: 10.1002/2014GC005436.

Connolly, J. A. D., 2010. The mechanics of metamorphic fluid expulsion. Elements, 6, 165–172.

Cox, S. F., 2010. The application of failure mode diagrams for exploring the roles of fluid pressure and stress states in controlling styles of fracture-controlled permeability enhancement in faults and shear zones. Geofluids, 10, 217–233.

De Mets, C., Gordon, R. G., and Argus, D. F., 2010. Geologically current plate motions. Geophysical Journal International, 181, 1–80.

Eberhart-Phillips, D., Chadwick, M., and Bannister, S., 2008. Three-dimensional attenuation structure of central and southern South Island, New Zealand, from local earthquakes. Journal of Geophysical Research, 113, B05308, doi: 10.1029/2007/JB005359.

Etheridge, M. A., 1983. Differential stress magnitudes during regional deformation and metamorphism: upper bound imposed by tensile fracturing. Geology, 11, 231–234.

Etheridge, M. A., Daczko, N. R., Chapman, T., and Stuart, C. A., 2020. Mechanisms of melt extraction during lower crustal partial melting. Journal of Metamorphic Geology, doi: 10.1111/jmg.12561.

Fagereng, Å., and Diener, J. F. A., 2011a. Non-volcanic tremor and discontinuous slab dehydration. Geophysical Research Letters, 38, L15302, doi:10.1029/2011GL048214.

Fagereng, Å., and Diener, J. F. A., 2011b. San Andreas Fault tremor and retrograde metamorphism. Geophysical Research Letters, 38, L23303, doi:10.1029/2011GL049550.

Fagereng, Å., Hillary, G. W. B., and Diener, J. F. A., 2014. Brittle-viscous deformation, slow slip, and tremor. Geophysical Research Letters, doi: 10.1002/2014GL060433.

Fagereng, Å., Diener, J. F. A., Meneghini, F., Harris, C., and Kvadsheim, A., 2018. Quartz vein formation by local dehydration embrittlement along the deep, tremorgenic subduction thrust interface. Geology, 46, 67–70.

Grapes, R., and Watanabe, T., 1992. Metamorphism and uplift of Alpine Schist in the Franz Josef–Fox glacier area of the Southern Alps, New Zealand. Journal of Metamorphic Geology, 10, 171–180.

Grapes, R., and Watanabe, T., 1984. Al–Fe^{3+} and Ca–Sr^{2+} epidotes in metagreywacke–quartzofeldspathic schist, Southern Alps, New Zealand. American Mineralogist, 69, 490–498.

Grapes, R., 1995. Uplift and exhumation of Alpine Schist, Southern Alps, New Zealand: thermobarometric constraints. New Zealand Journal of Geology and Geophysics, 38, 525–533.

Gray, D. R., and Foster, D. A., 2004. $^{40}Ar/^{39}Ar$ thermochronologic constraints on deformation, metamorphism and cooling/exhumation of a Mesozoic accretionary wedge, Otago Schist, New Zealand. Tectonophysics, 385, 181–210.

Guiraud, M., Powell, R., and Rebay, G., 2001. H_2O in metamorphism and unexpected behaviour in the preservation of metamorphic mineral assemblages. Journal of Metamorphic Geology, 19, 445–454.

Heron, D. W., 2018. Geological Map of New Zealand 1:250000. GNS Science Geological Map 1 (22nd ed). Lower Hutt, New Zealand. GNS Science.

Hetényi, G., Channard, K., Baumgartner, L. P., and Herman, F., 2020. Metamorphic transformation rate over large spatial and temporal scales constrained by geophysical data and coupled modelling. Journal of Metamorphic Geology, doi: 10.1111/jmg.12604.

Hobbs, B. E., and Ord, A., 2018. Coupling of fluid flow to permeability development in mid- to upper-crustal environments: a tale of three pressures. *In* Gessner, K., Blenkinsop, T. G. & Sorjonen-Ward, R., eds., Characterisation of ore-forming systems from geological, geochemical and geophysical studies. Geological Society, London, Special Publications, 453, 81–120.

Holland, T. J. B., and Powell, R., 2011. An improved and extended internally consistent thermodynamic dataset for phases of petrological interest, involving a new equation of state for solids. Journal of Metamorphic Geology, 29, 333–383. Doi: 10.1111/j.1525-1314.2010.00923

Koons, P. O., Craw, D., Cox, S. C., Upton, P., Templeton, A. S., and Chamberlain, C. P., 1998. Fluid flow during active oblique convergence: a Southern Alps model from mechanical and geochemical observations. Geology, 26, 159–162.

Little, T. A., Holcombe, R. J., and Ilg, B. R., 2002. Ductile fabrics in the zone of active oblique convergence near the Alpine Fault, New Zealand: identifying the neotectonics overprint. Journal of Structural Geology, 24, 193–217.

Little, T. A., Cox, S., Vry, J. K., and Batt, G., 2005. Variations in exhumation level and uplift rate along the oblique-slip Alpine Fault, central Southern Alps, New Zealand. GSA Bulletin, 117, 707–723.

Menzies, C. D., Teagle, D. A. H., Niedermann, S., Cox, S. C., Craw, D., Zimmer, M., Cooper, M. J., and Erzinger, J., 2016. The fluid budget of a continental plate boundary fault: quantification from Alpine Fault, New Zealand. Earth and Planetary Science Letters, 445, 125–135.

Mortimer, N., 2004. New Zealand's geological foundations. Gondwana Research, 7, 261–272.

Norris, R. J., Koons, P. O., and Cooper, A. F., 1990. The obliquely convergent plate boundary in the South Island of New Zealand: implications for ancient collision zones, New Zealand. Journal of Structural Geology, 12, 715–725.

Obara, K., 2002. Non-volcanic deep tremor associated with subduction in southwest Japan. Science, 296, 1679–1681.

Powell, R., Evans, K. A., Green, E. C. R., and White, R. W., 2019. The truth and beuty of chemical potentials. Journal of Metamorphic Geology, doi: 10.1111/jmg.12484.

Ring, U., Glodny, J., Angiboust, S., Little, T., and Lang, K. A. 2019. Middle to Late Miocene age for the end of amphibolite-facies mylonitization of the Alpine Schist, New Zealand: implications for onset of transpression across the Alpine Fault. Tectonics, 38, 4335–4359.

Shelly, D. R., Beroza, G. C., and Ide, S., 2007. Non-volcanic tremor and low-frequency earthquake swarms. Nature, 446, 305–307.

Stern, T., Okaya, D., Kleffmann, S., Scherwath, M., Henrys, S., and Davey, F., 2007. Geophysical exploration and dynamics of the Alpine Fault Zone. *In* A Continental Plate Boundary: tectonics at South Island, New Zealand. Geophysical Monograph Series, 175, doi: 10.1029/175GM11.

Tenczer, V., Powell, R., and Stüwe, K. 2006. Evolution of H_2O content in a polymetamorphic terrane: the Plattengneiss Shear Zone (Koralpe Austria). Journal of Metamorphic Geology, 24, 281–295.

Thomas, A. M., Nadeau, R. M., and Bürgmann, R., 2009. Tremor-tide correlations and near-lithostatic pore-pressure on the deep San Andreas fault. Nature, 462, 1048–1051.

Toy, V. G., Craw, D., Cooper, A. F., and Norris, R. J., 2010. Thermal regime in the central Alpine Fault zone, New Zealand: constraints from microstructures, biotite chemistry and fluid inclusion data. Tectonophysics, 485, 178–192.

Vry, J., Storkey, A. C., and Harris, C., 2001. Role of fluids in metamorphism of the Alpine Fault Zone, New Zealand. Journal of Metamorphic Geology, 19, 21–31.

Vry, J., Baker, J., Maas, R., Little, T. A., Grapes, R., and Dixon, M., 2004. Zoned (Cretaceous and Cenozoic) garnet and the timing of high-grade metamorphism, Southern Alps, New Zealand. Journal of Metamorphic Geology, 22, 137–157.

Vry, J., Powell, R., and Williams, J., 2008. Establishing the *P–T* path for Alpine Schist, Southern Alps near Hokitika, New Zealand. Journal of Metamorphic Geology, 26, 81–97.

Vry, J., Powell, R., Golden, K. M., and Petersen, K., 2010. The role of exhumation in metamorphic dehydration and fluid production. Nature Geoscience, **3**, doi: 10.1038/NGEO699.

Walther, J. V., and Orville, P. M., 1982. Volatile production and transport in regional metamorphism. Contributions to Mineralogy and Petrology, 79, 252–257.

Wannamaker, P. E., Jiracek, G. R., Stodt, J. A., Caldwell, G., Gonzalez, V. M., McKnight, D., and Porter, A. D., 2002. Fluid generation and pathways beneath an active compressional orogen, the New Zealand Southern Alps, inferred from magnetotelluric data. Geophysical Research Letters, 107, B6, doi:10.1029/2001JB000186.

Wech, A. G., Boese, C. M., Stern, T. A., and Townend, J., 2012. Tectonic tremor and deep slow slip on the Alpine Fault. Geophysical Research Letters, 39, L10303, doi:10.1029/2012GL051751.

Wech, A. G., Sheehan, A. F., Boese, C. M., Townend, J., Stern, T. A., and Collins, J. A. (2013). Tectonic tremor recorded by ocean bottom seismometers. *Seismological Research Letters*, 84, 752–758.

Wightman, R. H., Prior, D. J., and Little, T. A., 2006. Quartz vein deformed by diffusion creep-accommodated grain boundary sliding during a transient, high strain-rate event in the Southern Alps, New Zealand. Journal of Structural Geology, 28, 902–918.

Yardley, B. W. D., 1981. Effect of cooling on the water content and mechanical behaviour of metamorphosed rocks. Geology, 9, 405–408.